

This work was written as part of one of the author's official duties as an Employee of the United States Government and is therefore a work of the United States Government. In accordance with 17 U.S.C. 105, no copyright protection is available for such works under U.S. Law. Access to this work was provided by the University of Maryland, Baltimore County (UMBC) ScholarWorks@UMBC digital repository on the Maryland Shared Open Access (MD-SOAR) platform.

Please provide feedback

Please support the ScholarWorks@UMBC repository by emailing scholarworks-group@umbc.edu and telling us what having access to this work means to you and why it's important to you. Thank you.

All-optical bistability and switching near the Dirac point of a 2-D photonic crystal.

Nadia Mattiucci,¹ Mark J. Bloemer,² and Giuseppe D'Aguanno^{1,*}

¹*AEgis Tech., Nanogenesis Division 410 Jan Davis Dr, Huntsville, AL 35806, USA*

²*Dept. of the Army, Charles M. Bowden Facility, Redstone Arsenal, AL 35898, USA*
**giuseppe.daguanno@us.army.mil or gdaguanno@nanogenesisgroup.com*

Abstract: We investigate all-optical switching at the guided mode resonances originating near the Dirac point of a finite, 2-D photonic crystal consisting of a square lattice of dielectric columns possessing a cubic nonlinearity. The peculiar field localization properties of these Dirac-point guided mode resonances conspire to yield extremely low switching threshold at near-to-normal incidence for remarkably low filling factors of the nonlinear material.

©2013 Optical Society of America

OCIS codes: (160.5298) Photonic crystals; (230.4320) Nonlinear optical devices; (999.9999) Graphene-like photonic materials.

References and links

1. E. Yablonovitch, "Inhibited spontaneous emission in solid-state physics and electronics," *Phys. Rev. Lett.* **58**(20), 2059–2062 (1987).
2. S. John, "Strong localization of photons in certain disordered dielectric superlattices," *Phys. Rev. Lett.* **58**(23), 2486–2489 (1987).
3. J. D. Joannopoulos, R. D. Meade, and J. N. Winn, *Photonic Crystals, Molding the Flow of Light*. (Princeton University, 1995).
4. J. M. Lourtioz, H. Benisty, V. Berger, J.-M. Gérard, D. Maystre, and A. Tchebnokov, *Photonic Crystals*, (Springer, 2005).
5. A. Scherer, T. Yoshie, M. Loncar, J. Vuckovic, and K. Okamoto, "Photonic Crystal Nanocavities for Efficient Light Confinement and Emission," *J. Korean Phys. Soc.* **42**, 768–773 (2003).
6. J. C. Knight, T. A. Birks, P. S. Russell, and D. M. Atkin, "All-silica single-mode optical fiber with photonic crystal cladding," *Opt. Lett.* **21**(19), 1547–1549 (1996).
7. J. D. Joannopoulos, P. R. Villeneuve, and S. H. Fan, "Photonic crystals: putting a new twist on light," *Nature* **386**(6621), 143–149 (1997).
8. S. N. Tandon, M. Soljacic, G. S. Petrich, J. D. Joannopoulos, and L. A. Kolodziejski, "The superprism effect using large area 2D-periodic photonic crystal slabs," *Photonics Nanostruct. Fundam. Appl.* **3**(1), 10–18 (2005).
9. K. S. Novoselov, A. K. Geim, S. V. Morozov, D. Jiang, M. I. Katsnelson, I. V. Grigorieva, S. V. Dubonos, and A. A. Firsov, "Two-dimensional gas of massless Dirac fermions in graphene," *Nature* **438**(7065), 197–200 (2005).
10. A. H. Neto, F. Guinea, N. M. R. Peres, K. S. Novoselov, and A. K. Geim, "The electronic processes of graphene," *Rev. Mod. Phys.* **81**(1), 109–162 (2009).
11. F. D. M. Haldane and S. Raghu, "Possible Realization of Directional Optical Waveguides in Photonic Crystals with Broken Time-Reversal Symmetry," *Phys. Rev. Lett.* **100**(1), 013904 (2008).
12. S. Raghu and F. D. M. Haldane, "Analogues of quantum-Hall-effect edge states in photonic crystals," *Phys. Rev. A* **78**(3), 033834 (2008).
13. R. A. Sepkhanov, Ya. B. Bazaliy, and C. W. J. Beenakker, "Extremal transmission at the Dirac point of a photonic band structure," *Phys. Rev. A* **75**(6), 063813 (2007).
14. X. Zhang, "Observing *Zitterbewegung* for Photons near the Dirac Point of a Two-Dimensional Photonic Crystal," *Phys. Rev. Lett.* **100**(11), 113903 (2008).
15. M. Diem, T. Koschny, and C. M. Soukoulis, "Transmission in the vicinity of the Dirac point in hexagonal photonic crystals," *Physica B* **405**(14), 2990–2995 (2010).
16. X. Huang, Y. Lai, Z. H. Hang, H. Zheng, and C. T. Chan, "Dirac cones induced by accidental degeneracy in photonic crystals and zero-refractive-index materials," *Nat. Mater.* **10**(8), 582–586 (2011).
17. K. Sakoda, "Double Dirac cones in triangular-lattice metamaterials," *Opt. Express* **20**(9), 9925–9939 (2012).
18. G. D'Aguanno, N. Mattiucci, C. Conti, and M. J. Bloemer, "Field localization and enhancement near the Dirac point of a finite defectless photonic crystal," *Phys. Rev. B* **87**(8), 085135 (2013).
19. L. Li, "Formulation and comparison of two recursive matrix algorithms for modeling layered diffraction gratings," *J. Opt. Soc. Am. A* **13**(5), 1024–1035 (1996).

20. G. D'Aguanno, M. Centini, M. Scalora, C. Sibilia, Y. Dumeige, P. Vidakovic, J. A. Levenson, M. J. Bloemer, C. M. Bowden, J. W. Haus, and M. Bertolotti, "Photonic band edge effects in finite structures and applications to $\chi(2)$ interactions," *Phys. Rev. E* **64**, 16609 (2001).
 21. P. Vicent, N. Paraire, M. Neviere, A. Koster, and R. Reinisch, "Gratings in nonlinear optics and optical bistability," *J. Opt. Soc. Am. B* **2**(7), 1106–1116 (1985).
 22. Y. S. Kivshar and G. P. Agrawal, *Optical Solitons* (Academic, 2003).
 23. V. Ta'eed, N. J. Baker, L. Fu, K. Finsterbusch, M. R. E. Lamont, D. J. Moss, H. C. Nguyen, B. J. Eggleton, D. Y. Choi, S. Madden, and B. Luther-Davies, "Ultrafast all-optical chalcogenide glass photonic circuits," *Opt. Express* **15**(15), 9205–9221 (2007).
 24. V. Mizrahi, K. W. Delong, G. I. Stegeman, M. A. Saifi, and M. J. Andrejco, "Two-photon absorption as a limitation to all-optical switching," *Opt. Lett.* **14**(20), 1140–1142 (1989).
-

1. Introduction

Photonic crystals (PCs) or photonic band gap structures (PBGs) [1–5] have opened novel venues to control light localization at the nanoscale level and to enhance light-matter interactions in an unparalleled way. Any nonlinear phenomena, such as Raman scattering, quantum-dot and quantum-well emission, nonlinear harmonic generation, all-optical switching, just to name few, can in principle benefit from the high degree of light localization achievable in these structures. Among the numerous applications of PCs, we cite photonic crystal fibers [6], photonic crystal circuits [7] and photonic crystal super-prism structures [8]. The recent discovery of graphene [9], a purely two-dimensional electronic system where the conduction band and the valence band touch each other at the Dirac point leading to remarkable electronic transport properties [10], has sparked a renewed interest in the study of Dirac points in 2-D PCs [11–17]. In the case of PCs, two photonic bands touch as a pair of cones (Dirac cones) giving rise to a linear, instead of a parabolic, dispersion for photons. In a recent publication [18] we have studied the anomalous field localization properties in the stop band of a linear, 2-D PC made of an array of dielectric columns near its Dirac point. At normal incidence the crystal exhibits a Dirac point with 100% transmission. At angles slightly off the normal where the crystal is 100% reflective, instead of exponentially decaying fields as in a photonic stop band, the field becomes strongly localized and enhanced inside the crystal. We have explained that this anomalous localization is due to guided mode resonances (GMRs) that are the foundation of the Dirac point itself and also shape its adjacent band gap. In this work the anomalous localization properties and strong field enhancement near the Dirac point are used to boost Kerr nonlinearities and achieve switching and bistable response for low input intensities and low filling factor of the nonlinear material. In Section 2 we detail the main results of our study followed by a discussion and in Section 3 we present our conclusions.

2. Results and discussion

We start our analysis by showing in Fig. 1 the structure under investigation.

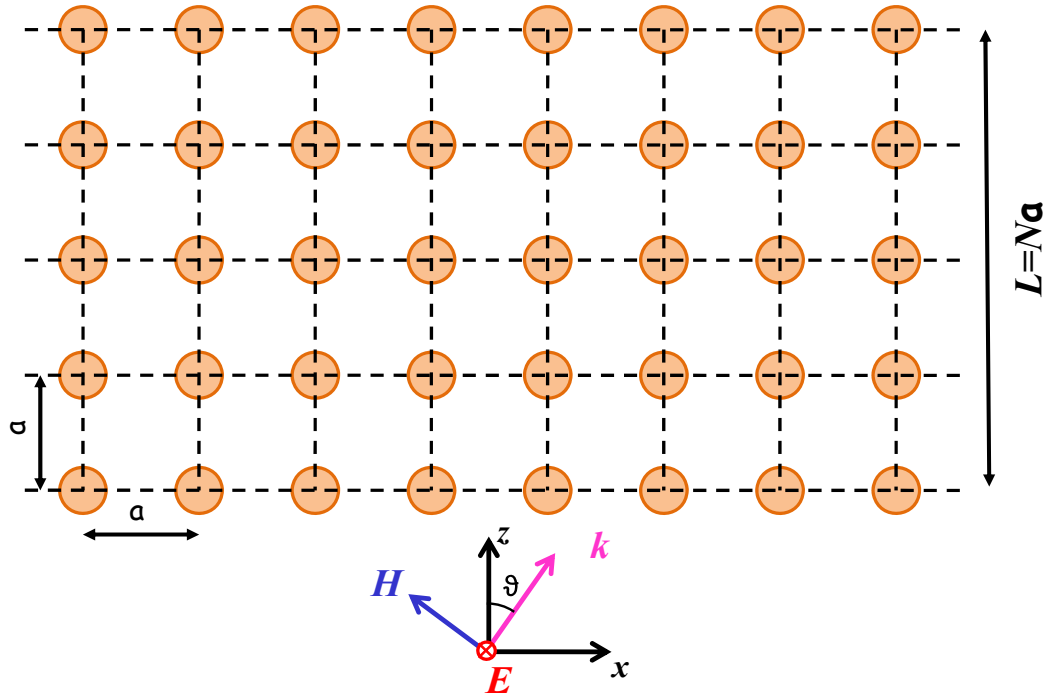


Fig. 1. Cross sectional view of a 2-D PC consisting of a square array (period a) of dielectric columns with radius r and relative permittivity ϵ . The structure possesses a finite number N of rows along the z -direction and a total length $L = Na$. We suppose that the columns are made of a nonlinear Kerr-type material with a generic cubic coefficient $\chi^{(3)}$. A plane electromagnetic wave with the electric field parallel to the axis of the columns is incident on the structure with its k -vector in the (x, z) plane (in-plane coupling) forming an angle ϑ with respect to the z -direction.

In Fig. 2 we show the photonic band gap structure in the (ω, k_x) plane for the following parameters: $N = 5$, $r/a = 0.2$, $\epsilon = 12.5$ [16,18]. The photonic band gap structure has been calculated through the transmittance, i.e. the transmitted power divided the incident power. The numerical calculation has been performed using an in-house developed code based on the Fourier-modal-method (FMM) [19].

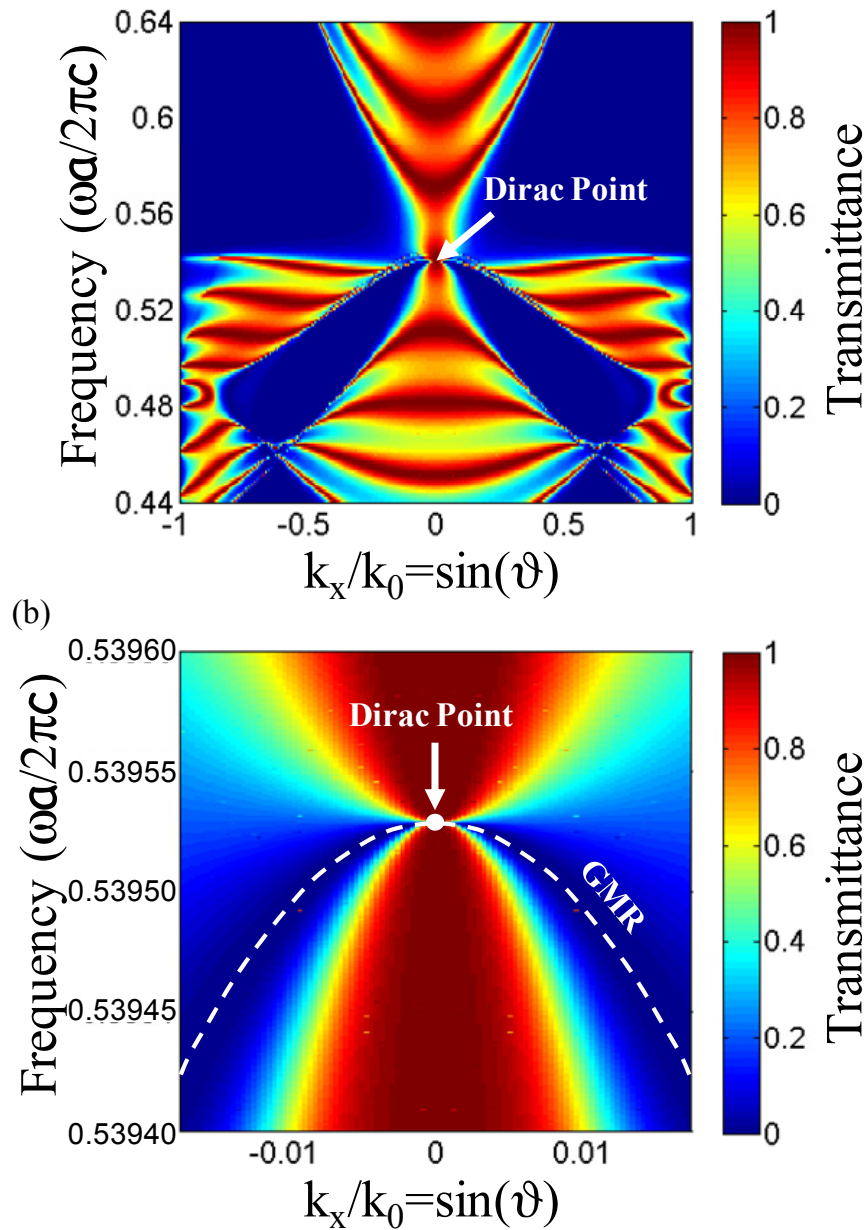


Fig. 2. (a) Transmittance in the (ω, k_x) plane. (b) Magnification of the transmittance around the Dirac point. The dashed line indicates the calculated dispersion of the Dirac-point GMR. The structure's parameters are: $N = 5$, $r/a = 0.2$, $\varepsilon = 12.5$.

In particular Fig. 2(a) shows the transmittance in the (ω, k_x) plane for a wide frequency range. From Fig. 2(a) it is noted the overall conical shape of both the upper and lower pass band that touch each other at the Dirac point located at $\omega a / 2\pi c \approx 0.54$. An additional lateral pass band is also present. It is important to underline that here we are dealing with a finite structure along z . The pass bands are actually characterized by multiple Fabry-Perot-like transmission resonances due to the multiple interference effects of the field reflected/transmitted from each of the N rows of columns the structure is made of. This is a

typical characteristic of finite PCs even in lower dimensional systems such as 1-D multilayered structures [20]. Figure 2(b) shows instead a magnification of the transmittance near the Dirac point of the structure and the dispersion of the corresponding Dirac-point GMR calculated according to [18]. The dispersion curve located in the band gap of the structure corresponds to sharp reflection resonances for close-to-normal incident conditions. As discussed at length in [18], the Dirac-point GMR is characterized by an exceptionally dispersive coupling strength as function of the incident angle: at close-to-normal incidence the electric field is extremely localized over the columns with localization enhancement factors exceeding 10^7 for $\vartheta \rightarrow 0^\circ$. As the incident wave departs from the close-to-normal condition the coupling strength of the GMR dramatically decreases marking the transition from localized modes to stop-band evanescent modes. In Fig. 3 we show, as an example, the localization of the electric field for an incident angle $\vartheta = 0.1^\circ$.

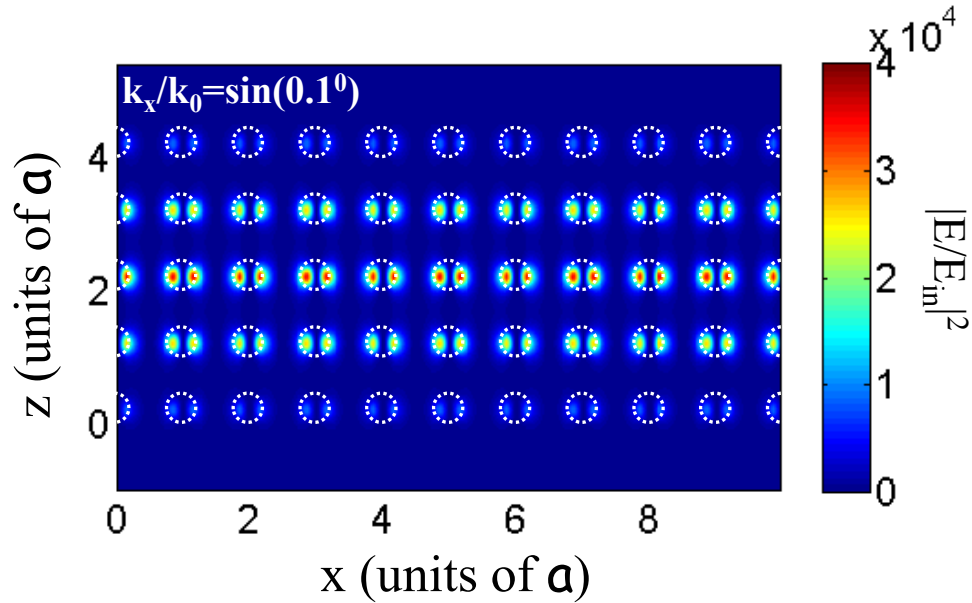


Fig. 3. Cross sectional view of the field localization in the stop-band at the Dirac-point GMR for $\vartheta = 0.1^\circ$. The dashed circles indicate the position of the columns.

The field is exceptionally squeezed inside the columns with a typical, dipolar-like localization profile. Localization enhancements exceeding 10^4 are noted in the central row. Those features are extremely well suited to boost the nonlinear properties of the columns. In this case we suppose that the columns possess a Kerr-type cubic nonlinearity so that their local nonlinear permittivity is dependent on the local field intensity following the usual relation: $\epsilon_{NL} = \epsilon + \chi^{(3)}|E|^2$. Figure 4 reports the results of the nonlinear transmittance as detailed in the figure caption. The nonlinear calculation has been performed using a mean field approach as in [21].

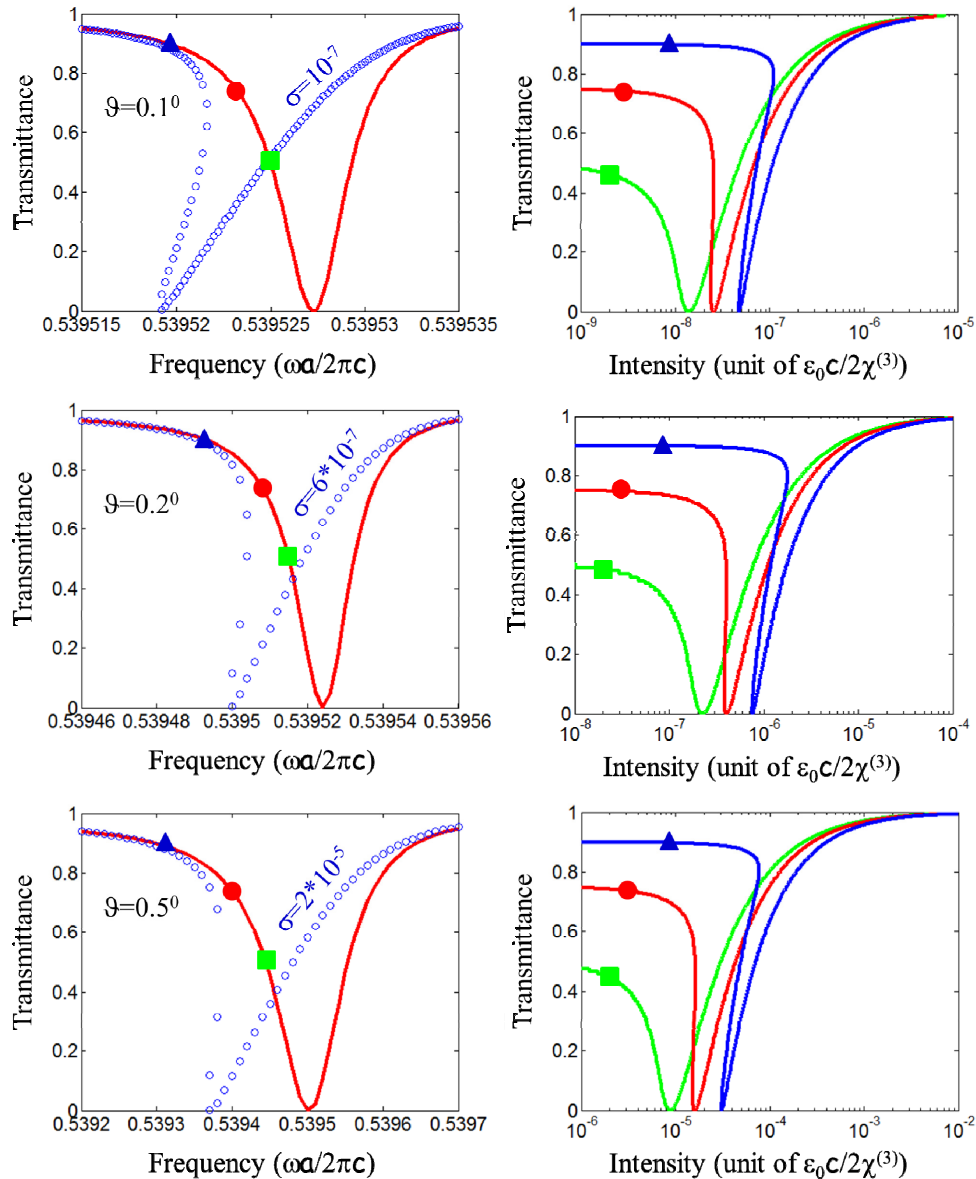


Fig. 4. (Left panel) Linear transmittance (red) and nonlinear transmittance (circles) with the onset of optical bistability for different incident angles along the Dirac-point GMR. The control parameter is $\sigma = 2\chi^{(3)} I_{in}/\epsilon_0 c$ where I_{in} is the input intensity, ϵ_0 the vacuum permittivity and c the speed of light in vacuo. The marks on the linear transmittance (triangle, circle, square) indicate the tuning conditions for the nonlinear calculations reported in the right panel. (Right panel) Nonlinear transmittance vs. input intensity for the incident angle reported in the left panel. Note the change in scale for the input intensity as the incident angle increases.

As expected, in agreement with the decrement of the field localization when the incident field departs from the close-to-normal condition, the threshold intensity for the onset of the optical bistability and switching increases for increasing incident angles. It is also interesting to note in the right panel how, depending on the tuning conditions on the linear resonance, the nonlinear transmittance passes from an optical limiting behavior (green curve and red curve) to a full hysteresis cycle (blue curve). To have an idea of the actual intensities needed to

achieve optical bistability and switching we provide in Table 1 a synoptic prospect which refers to the cubic nonlinearity of two widely used materials for nonlinear optical applications, namely silica and chalcogenide glasses. Silica is mainly used for temporal soliton propagation in optical fibers [22], while chalcogenide glasses are mainly used for nanoscale photonic applications [23] due to their extremely high cubic nonlinearity and low two-photon absorption. The cubic nonlinearity of many dielectric and semiconductor materials falls in between the range set by chalcogenide glasses and silica. It is worthwhile to note that the proper material choice should be done consistently with the known limitation to all-optical switching set by material's two-photon absorption [24].

Table 1.

σ	Chalcogenide $\chi^{(3)} = 4.4 \cdot 10^{-20} \text{ m}^2/\text{V}^2$	Silica $\chi^{(3)} = 3.4 \cdot 10^{-22} \text{ m}^2/\text{V}^2$
10^{-7}	$3 \cdot 10^5 \text{ W/cm}^2$	$3.9 \cdot 10^7 \text{ W/cm}^2$
$6 \cdot 10^{-7}$	$1.8 \cdot 10^6 \text{ W/cm}^2$	$2.3 \cdot 10^8 \text{ W/cm}^2$
$2 \cdot 10^{-5}$	$6 \cdot 10^7 \text{ W/cm}^2$	$7.8 \cdot 10^9 \text{ W/cm}^2$

The values of the control parameter refer to the three cases studied in the left panel of Fig. 4. For example, in the first case ($\sigma = 10^{-7}$) the corresponding input intensity for the onset of optical bistability is $\sim 0.3 \text{ MW/cm}^2$ for chalcogenide glasses and $\sim 40 \text{ MW/cm}^2$ for silica. In both cases we are speaking of extremely low intensity, well below the GW/cm^2 range typical of nonlinear optical phenomena. These results are even more remarkable if we consider that the filling factor of the nonlinear material (ratio between the area of the column and the area of the elementary cell) is in our case only $\sim 10\%$. The kind of resonances explored in this work require the use of a collimated light beam with an angular divergence $\Delta\vartheta \sim 0.1^\circ$ which, roughly speaking, corresponds to a beam waist $w_0 = \lambda/(\pi\Delta\vartheta) \sim 200\lambda$. This value of the beam waist is compatible, for example, with the degree of focusing necessary to obtain an intensity $\sim \text{GW/cm}^2$ from a Ti:sapphire laser at $\lambda = 800 \text{ nm}$.

3. Conclusions

In conclusion, we have studied all-optical switching at the Dirac-point GMR [18] and shown that extremely low switching intensities can be achieved even for structures in which the effective volume of the nonlinear material is remarkably small. This property may pave the way to a great variety of nonlinear devices such as: self-tunable optical sensing structures for laser eye protection, switches, optical memories, and advanced nanocircuits. In particular, the strong dependence of the Dirac-point GMR on the incident angle has applications in nonlinear angularly selective filters and collimators. Moreover, similar concepts may also be applied to harmonic generators and parametric amplifiers, which we plan to examine in future studies.

Acknowledgments

This work has been supported by DARPA SBIR project number W31P4Q-11-C-0109.